ADVANCING EARTH AND SPACE SCIENCES

JGR Space Physics

RESEARCH ARTICLE

10.1029/2024JA033167

Special Collection:
Space Weather Events of 2024 May 9-15

Nocturnal Sporadic Cusp-Type Layer (Es_c) Resulting From Anomalous Excess Ionization Over the SAMA Region During the Extreme Magnetic Storm on 11 May 2024

L. C. A. Resende[1,2], Y. Zhu[1,3], A. M. Santos[1,2], R. A. J. Chagas[2], C. M. Denardini[2], C. Arras[4,5], L. A. Da Silva[1,2,3], P. A. B. Nogueira[6,7], S. S. Chen[2], V. F. Andrioli[1,2], J. Moro[1,8], J. R. Costa[2], H. Li[1], C. Wang[1], and Z. Liu[1]

[1]State Key Laboratory for Space Weather, National Space Science Center, Chinese Academy of Sciences, Beijing, China, [2]National Institute for Space Research (INPE), São José dos Campos, Brazil, [3]University of Chinese Academy of Sciences, Beijing, China, [4]Helmholtz Centre Potsdam, German Research Centre for Geosciences (GFZ), Department 1: Geodesy and Remote Sensing, Potsdam, Germany, [5]Institute of Geodesy and Geoinformation Science, Berlin, Germany, [6]Federal Institute of Education, Science and Technology of São Paulo (IFSP), Jacareí, Brazil, [7]Brazil Joint Laboratory for Space Weather, NSSC/INPE, São José dos Campos, Brazil, [8]Southern Regional Space Research Center – COCRE/INPE, Santa Maria, Brazil

Key Points:

- Atypical Sporadic (Es) layer type was detected for the first-time during nighttime in the South American Magnetic Anomaly
- Digisonde data and simulations show the extra ionization that occurred in the main phase of the strong magnetic storm on 11 May 2024
- The E region presence enabled the formation of the cusp-type Es layer (Esc), which had only been seen during daytime periods until now

Correspondence to:
L. C. A. Resende,
laysa.resende@inpe.br;
laysa.resende@gmail.com

Citation:
Resende, L. C. A., Zhu, Y., Santos, A. M., Chagas, R. A. J., Denardini, C. M., Arras, C., et al. (2024). Nocturnal sporadic cusp-type layer (Es_c) resulting from anomalous excess ionization over the SAMA region during the extreme magnetic storm on May 11, 2024. *Journal of Geophysical Research: Space Physics*, *129*, e2024JA033167. https://doi.org/10.1029/2024JA033167

Received 10 AUG 2024
Accepted 1 NOV 2024

Abstract Digisonde data showed a peculiar behavior in the nighttime lower ionosphere over Cachoeira Paulista (CXP, 22.7°S, 45°W, dip ~35°), a low-latitude station located inside the South American Magnetic Anomaly (SAMA) during the main phase of the extreme magnetic storm on 11 May 2024. The E region appeared in observational data at high altitudes after sunset, which is unexpected. In sequence, it performed an unusual descending movement due to the disturbed electric field. The extra ionization responsible for forming the nocturnal E layer is due to the precipitation (EPP) of low energic (<30 keV) particles. Moreover, a diurnal cusp-type Es layer (Es_c) appeared simultaneously, which has never been reported in the literature at such hours. Thus, the results further suggest that the EPP may have caused an oscillation in the thermosphere, forming the Es_c usually seen in the daytime. Therefore, this study shows the different mechanisms acting together during this magnetic storm, creating a daytime ionosphere after sunset over the SAMA region, as confirmed by observational data and simulations.

1. Introduction

Sporadic E layers (Es) are zones of denser ionizations located at around 100–150 km altitude. They are classified into different types that are well-known in the literature, being divided according to the formation mechanism distinguished by lowercase letters in ionosonde data (ionograms) (Mathews, 1998; Resende et al., 2013; Whitehead, 1961). The Es layers are composed of molecular ions (O_2^+, NO^+, N_2^+, O^+) and mainly metallic ions, such as Fe^+ and Mg^+, that allow them to be continuously observed in data (Kopp, 1997). The main physical formation process at low- and midlatitudes refers to wind shear, characterized by the accumulation of charged particles at the null points of the zonal wind shear vertical profile (Haldoupis, 2011). Specifically, meridional and zonal components of the tidal winds (**U**) carry the ions horizontally, and the magnetic field (**B**) presence results in a vertical U**x**B force, creating a new layer at the location of the wind reversal. Electrons following the vertical magnetic field line maintain plasma neutrality. The daytime types "c" (cusp), "h" (high), "l" (low), and the nighttime "f" (flat) are found in ionograms over the low/mid-latitudes. Thus, layers of these types are formed by the wind shear mechanism.

Stations located in the Brazilian sector are of particular interest for the ionospheric investigation because of the presence of the South American Magnetic Anomaly (SAMA), characterized by a weak magnetic field intensity concerning the other global locations (Abdu et al., 1981, 2005; Batista & Abdu, 1977; Da Silva et al., 2022). Abdu et al. (1973) analyzed the interaction between the magnetosphere, the inner radiation belt, and ionosphere over SAMA, which was present closer to the Atlantic at that time but moved to Southern Brazilian regions such as Cachoeira Paulista (CXP, 22.7°S, 45°W, dip ~35°). The authors showed an azimuthal drift in the electron precipitation inside SAMA during the sudden commencement (SC) of the magnetic storm that occurred on 4 August 1972. Furthermore, the authors detected the absorption of the cosmic noise intensity (CNA - cosmic noise absorption) in riometer data, mainly observed in the same magnetic storm recovery phase. Later, Moro et al. (2012) investigated the CNA events using the South American Riometer Network (SARINET) operated inside the SAMA during the 3 September 2008, magnetic storm. The results are similar to those reported by Abdu et al. (1973), in which the CNA happened in the recovery phase.

The electron precipitation effect in the SAMA was also analyzed using ionosonde data. The main results are the occurrences of the auroral ("a") Es layer type (Es_a), spreading trace that can reach high-frequency values (Batista & Abdu, 1977; Moro et al., 2022). The Es_a layer is seen mainly in the magnetic storm recovery phase, as the CNA absorption mentioned before. The explanation for this behavior is still under discussion. Nonetheless, it is believed that the interaction process in the sun-magnetosphere-ionosphere in the inner radiation belt would be slower during the main magnetic storm phase since there are still processes in the outer radiation belt. In fact, Batista and Abdu (1977) and Da Silva et al. (2022) showed that the Es_a layer occurs due to a process called pitch angle diffusion in which the resonance of low-energy electrons with Hiss waves breaks the first invariant (magnetic moment invariant) and/or second invariant (longitudinal invariant). Thus, particles between 0.5 and 30 keV would enter the atmosphere, causing an abrupt ionization, forming this Es_a layer that is characteristic for auroral regions.

Abdu et al. (2005) studied the extra ionization process over the SAMA stations around the quiet period. Since the SAMA is a broad geographic region with lower geomagnetic field intensity than the rest of the globe, the entry of particles can occur continuously, explaining the increased conductivity in these regions. This process is called collisional, and it happens because low-energy electrons enter the SAMA region due to a lower mirror point (∼100 km). Thus, there is an interaction with ions and neutral particles at the E-region heights, increasing ionization. This process is called Coulomb scattering. During disturbed periods, this intensification is much higher, which causes an atypical E-region development at night (Santos et al., 2016). Therefore, the nighttime E region in ionograms indicates an increased ionization due to particle precipitation in SAMA during geomagnetic storms.

The Es layer formed by wind shear does not suffer significant influence during the disturbed periods and has its seasonal variations as seen in several works in the literature (Arras et al., 2008; Christakis et al., 2009; Conceição-Santos et al., 2019; Moro et al., 2023). In fact, the particle precipitation can cause the nocturnal E region or the Es_a layer. However, other Es layer types, such as "c", "f/l", and "h", are not modified due to this extra ionization since they are formed by metallic ions which the production and loss processes take a long time (Mathews, 1998) independently of the geomagnetic conditions. Also, Resende et al. (2021) show that the disturbed electric fields driven by Prompt Penetration Electric Field (PPEF) (Balan et al., 2008) and Disturbance Dynamo (DDEF) (Blanc & Richmond, 1980) do not affect the Es layer behavior over CXP.

This study analyzes the atypical Es_c layer presence during the nighttime period of the intense 10–11 May 2024, magnetic storm main phase. The Es_c layer appears as a continuous trace that starts from the E region and, for this reason, is not detected at night by Digisondes. The occurrence of the Es_c layer during this period has never been mentioned in the literature. We show that the extra ionization that occurred during this magnetic storm in the CXP region, which is located inside SAMA, triggered the detection of the E region. Also, it is believed that this additional electron that entered the atmosphere caused oscillations in the plasma, enabling the Es_c layer formation. Furthermore, the E region had an abrupt descent, meaning that different mechanisms were acting besides the extra ionization, such as disturbed electric fields. We also used an E/Es layer numerical model with a novel particle precipitation input to prove that this unusual behavior over the CXP region is due to the extra ionization. Finally, this work will discuss all these nocturnal processes during this disturbed period that may have contributed to atypical phenomena in the SAMA region.

2. Data Set and Modeling

2.1. Digisonde Data

In this study, we used the data obtained from a radar that operates in high frequency (HF 3–30 MHz), a digital ionosonde. Specifically, the digital ionosonde used in this work is a Digisonde Portable Sounder— 4D (DPS-4D) that transmits radio waves continuously in a 10-min time resolution. The echoes captured by the receiver antennas are shown through frequency-by-virtual height graphs called ionograms. Through the ionograms, it is possible to observe the E and F regions as well as the Es layers using the SAO-Explorer program that contains the Automatic Real-Time Ionogram Scaler (ARTIST) software to interpret the data. Thus, it is possible to obtain the Es layer

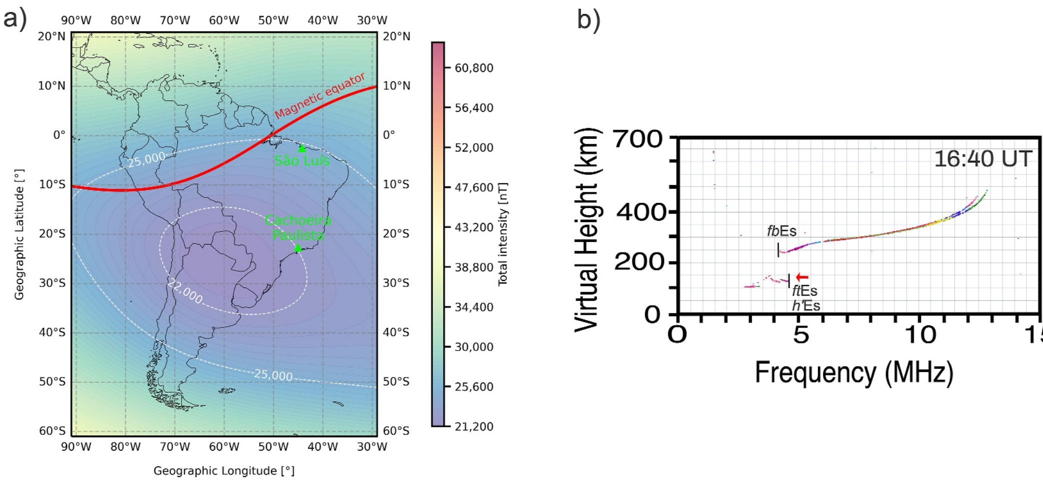

Figure 1. (a) Map showing the low magnetic field values over the Brazilian stations, 22,000 nT for Cachoeira Paulista, and 25,000 nT for São Luís, characterizing the SAMA stations, (b) example of an ionogram over CXP at 1640 UT on 10th May 2024, showing the diurnal Es_c layer and frequencies (*ft*Es and *fb*Es) and height (*h'*Es) parameters.

frequencies, the *fb*Es (blanketing frequency), the frequency point in the upper ionospheric layer where the Es layer blocks the transmitted electromagnetic signal, and the *ft*Es (top frequency) characterized by the maximum frequency trace of the Es layer, and the virtual height of the Es layer (*h'*Es). Additionally, it is possible to classify the different types of existing Es layers, such as "c", "a", "l/f", "h", and others, defined by the Union of Radio Science (URSI Handbook) related to their formation mechanisms (Piggott & Rawer, 1978). More details about the Digisonde and Es layer classification can be found in Reinisch et al. (2009) and Resende et al. (2013).

The map in Figure 1a shows the Digisonde locations in CXP and São Luís (SLZ, 2.3°S, 44.2°W, dip ~8°) (green triangles), the geomagnetic equator position (red line), and the white isolines indicate the magnetic field value calculated by the International Geomagnetic Reference Field (IGRF) model in 2024 (22,000 nT for CXP and 25,000 for SLZ), illustrating the stations inside the SAMA. Notice that the magnetic field values around the southern of Brazilian stations were lower than other global regions, as seen in the color bars in this figure. To exemplify the typical behavior in quiet times, we show the Es_c layer type in ionogram (red arrow) at 1640 UT (13:40 LT) over CXP on 10 May 2024, hours before the magnetic storm occurrence (Figure 1b). As mentioned before, the Es_c layer occurrence is conditioned to the E region presence, which is detected in the daytime. This ionogram also contains the *fb*Es (4.2 MHz), *ft*Es (4.6 MHz), and *h'*Es (118 km) parameters (black lines).

2.2. The Inclusion of Particle Precipitation Effects in the MIRE Model

The E Region Ionospheric Model (MIRE, in Portuguese) was created by Carrasco et al. (2007) and modified by Resende et al. (2017) to simulate the electron density (*Ne*) of the E region and the Es layer over the Brazilian stations. Currently, MIRE simulates the ionosphere between 86 and 140 km of height with a step of 0.2 km and a time resolution of 2 min. This model solves the continuity and momentum equations for the main E region ions (NO^+, O_2^+, N_2^+, O^+). The metallic ions Fe^+ and Mg^+ are included to reproduce the Es layer. The electron density *Ne* is obtained by:

$$N_e = [NO^+] + [O_2^+] + [O^+] + [N_2^+] + [Fe^+] + [Mg^+] \tag{1}$$

The numerical solution for each ion in Equation 1 is based on the continuity that depends on the production, loss, and transport terms. The transport term in MIRE is the ions' vertical velocity (V_{iz}):

$$V_{iz} = \frac{\omega_i^2}{(\nu_{in}^2 + \omega_i^2)}\Bigg[\cos I \cdot \sin I \cdot U_X + \frac{\nu_{in}}{\omega_i} \cdot \cos I \cdot U_y + \frac{1}{\nu_{in}}\frac{e}{m_i} \cdot \cos I \cdot \sin I \cdot E_x + \frac{e}{\omega_i m_i} \cdot \cos I \cdot E_y$$
$$+ \frac{e}{\nu_{in} m_i} \cdot \left(\frac{\nu_{in}^2}{\omega_i^2} + \sin^2 I\right) \cdot E_z\Bigg], \tag{2}$$

where v_{in} is the ion-neutral collision frequency, I is the magnetic inclination angle, ω_i is the ion gyrofrequency, m_i represents the mass of the ion, and e stands for the electric charge of the ion. The E_x, E_y, and E_z are the electric field components. They become an important factor controlling the ion motion in some specific cases, such as disturbed periods or close to the magnetic equator as explained in Resende et al. (2021).

Extra ionization occurred at nighttime over SAMA due to energetic electron precipitation. To analyze this effect, we implemented a parametrization in MIRE to describe the ionization rate caused by the particle precipitation. Hence, MIRE now considers the production of electron-ion pairs at all the simulated heights. As we will observe in the results, the inclusion of this effect transforms MIRE into an important tool for analyzing particle precipitation effects in SAMA during space weather events.

We used the parametrization described by Fang et al. (2010) and discussed by Da Silva et al. (2022), which is based on satellite data. The parametric model computes the total ionization rate (cm^{-3} s^{-1}) at a specific altitude for each energy level (keV), given an incident electron energy flux $\boldsymbol{Q_m(\varepsilon)}$ (keV cm^{-2} s^{-1}). We selected the best-fit Maxwellian function in Fang et al. (2010) to model the latter, represented by:

$$Q_m(\varepsilon) = \frac{Q_o}{2{E_o}^3} E \exp\left(-\frac{E}{E_o}\right), \tag{3}$$

where Q_o is the total energy flux (keV cm^{-2} s^{-1}), E_o is the best-fit characteristic energy (keV), selected as 7.1 keV, and E is the energy range that precipitates in the E region, which varies from 0.5 to 30 keV. The selected value of Q_o in Fang et al. (2010) that produced the best-fit results compared to the standard model was 1 erg (or 6. 242 $\times 10^8$ keV). In this work, we adjusted Q_o to obtain the nighttime density in MIRE that matches the observational data. Hence, we could infer the total energy flux in the ionosphere during the studied period.

3. Results

3.1. Synopsis of the Extreme Event on 10–11 May 2024

The most intense magnetic storm of the solar cycle 25 until today occurred recently and was caused by multiple Interplanetary Coronal Mass Ejections (ICMEs) incidents on the Earth on 10–11 May 2024, reaching the G5 level (extreme event). Figure 2 shows the overview of the interplanetary conditions and ground-based magnetic indices between 10 and 12 May 2024. These ICMEs caused a strong geomagnetic storm (Gonzalez et al., 1994; Tsurutani et al., 1995) that directly affected the ionosphere. The parameters are the interplanetary magnetic field Z component (IMF B_z—panel a), the magnetopause standoff distance (R_{mp}—panel b) from Shue et al. (1998) model, the SME index (panel c) obtained from the SuperMAG magnetometer network data, which is, in turn, equivalent to the Auroral Electrojet, and the SYM-H index (panel d) to show the disturbance storm time. The interplanetary medium conditions at the L1 Lagrangian point were obtained from OmniWeb database (https://omniweb.gsfc.nasa.gov/index.html), and the SME and SYM-H indices were derived from magnetometers data and available at https://supermag.jhuapl.edu/indices and https://wdc.kugi.kyoto-u.ac.jp, respectively.

The IMF B_z component had a southward direction with a minimum value of −41 nT at 00:45 UT on 11 May 2024, favoring the magnetospheric convection electric field penetration (Abdu, 1997). These disturbed electric fields, known as undershielding, penetrate the auroral regions, and they are propagated through transverse waveguide modes (TMO) along magnetic field lines, reaching and influencing the ionosphere of low latitudes and equatorial regions (Kikuchi, 2005). This electric field from the undershielding process is eastward during the day and westward during the night. As seen in Figure 2a, the IMF B_z recovered after the minimum value (around 02:30 UT) and returned to the north direction at ~06:00 UT, which helped the establishment of the overshielding electric field, meaning that the electric fields had the opposite direction to the undershielding process (westward during the day and eastward during the night). The red line refers to the beginning occurrence of the Es_c layer at 02:00 UT on 11 May 2024, which will be discussed later.

Figure 2b shows the R_{mp}, which achieved ~a 5 Earth radius (R_E ~6,371 km), implying a significant magnetosphere compression that lasted up to 11 May 2024, at 12:00 UT. It means that a considerable amount of energy entered the Earth's atmosphere, causing modifications in the ionosphere behavior at all latitudes (Abdu, Kherani, Batista, & Sobral, 2009; Abdu et al., 2006; Balan et al., 2008; Batista et al., 1991; Sobral et al., 2001). One of these changes in the ionosphere is the electron particle precipitation driven by radiation belts (Da Silva et al., 2022). The

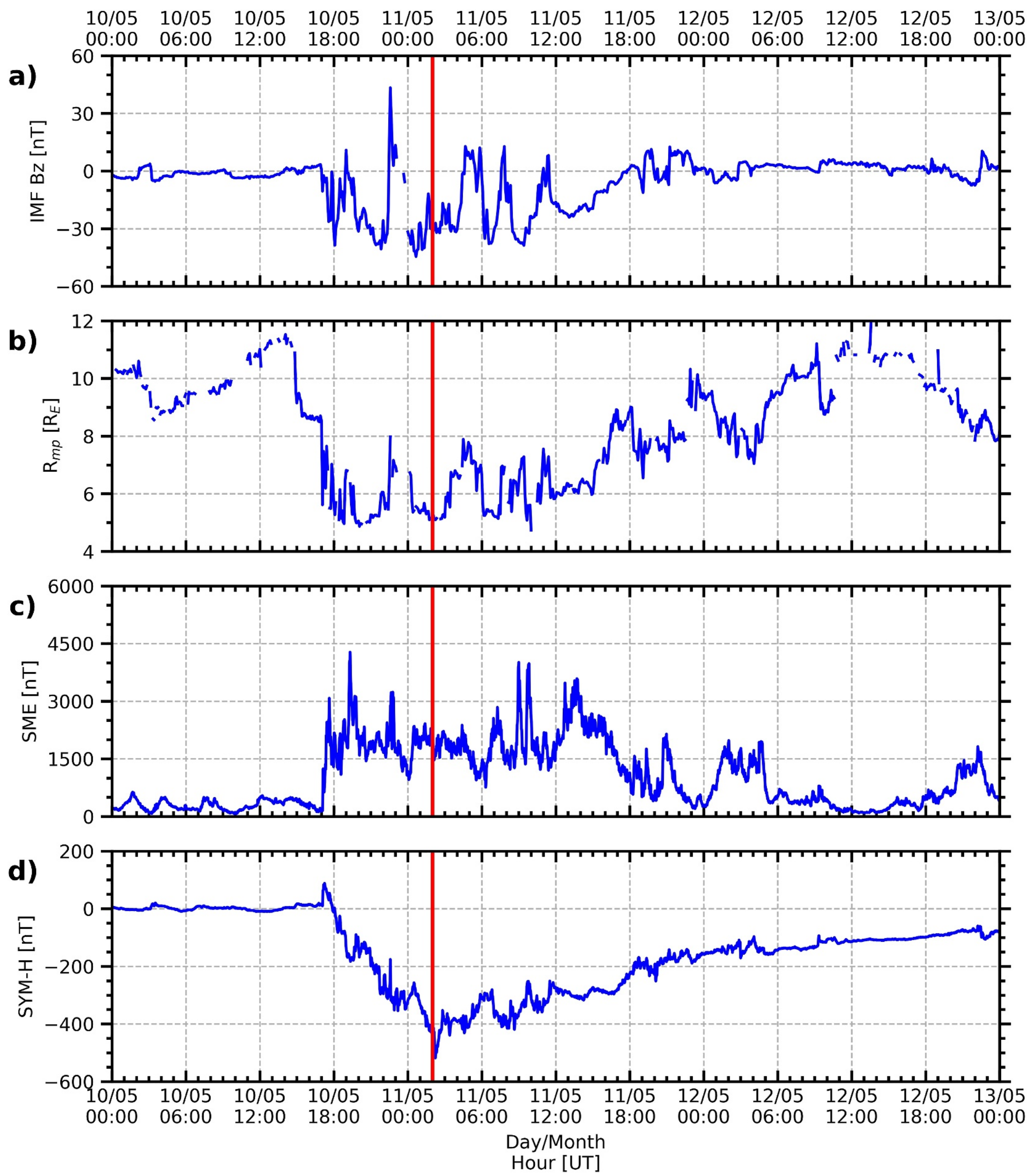

Figure 2. Three-days overview of interplanetary conditions and ground-based magnetic indices from May 10 to 12, 2024, (a) The interplanetary magnetic field component B_z, (b) the magnetopause standoff distance R_{mp}, (c) the SME index, and (d) the SYM-H index.

significant increase in the SME index values greater than 4,000 nT indicates a substantial energetic particle quantity infiltrated the auroral regions. This condition probably allowed the disturbed electric fields to penetrate and activate the ionospheric dynamo. The SYM-H index, highlighting the ICME arrivals in the Earth's magnetosphere on 10 May 2024, caused a Sudden Storm Commencement (SSC) at 1715 UT of 88 nT. This figure shows that the SYM-H reached −518 nT at 0214 UT on 11 May 2024. A feature of this magnetic storm is that the energization of the ring current was so intense and fast during this extreme event that the decrease of the SYM-H index after the SSC was very abrupt. Thus, the negative values of this index lasted until days after the main phase of the magnetic storm.

3.2. The Nighttime E Region and Es_c Layer Occurrences Over SAMA

The E region is a layer that follows the behavior of a Chapman layer in which the electronic density depends on the cosine of the zenith angle. The continuity equation calculates the electron density profile in which chemical

10.1029/2024JA033167

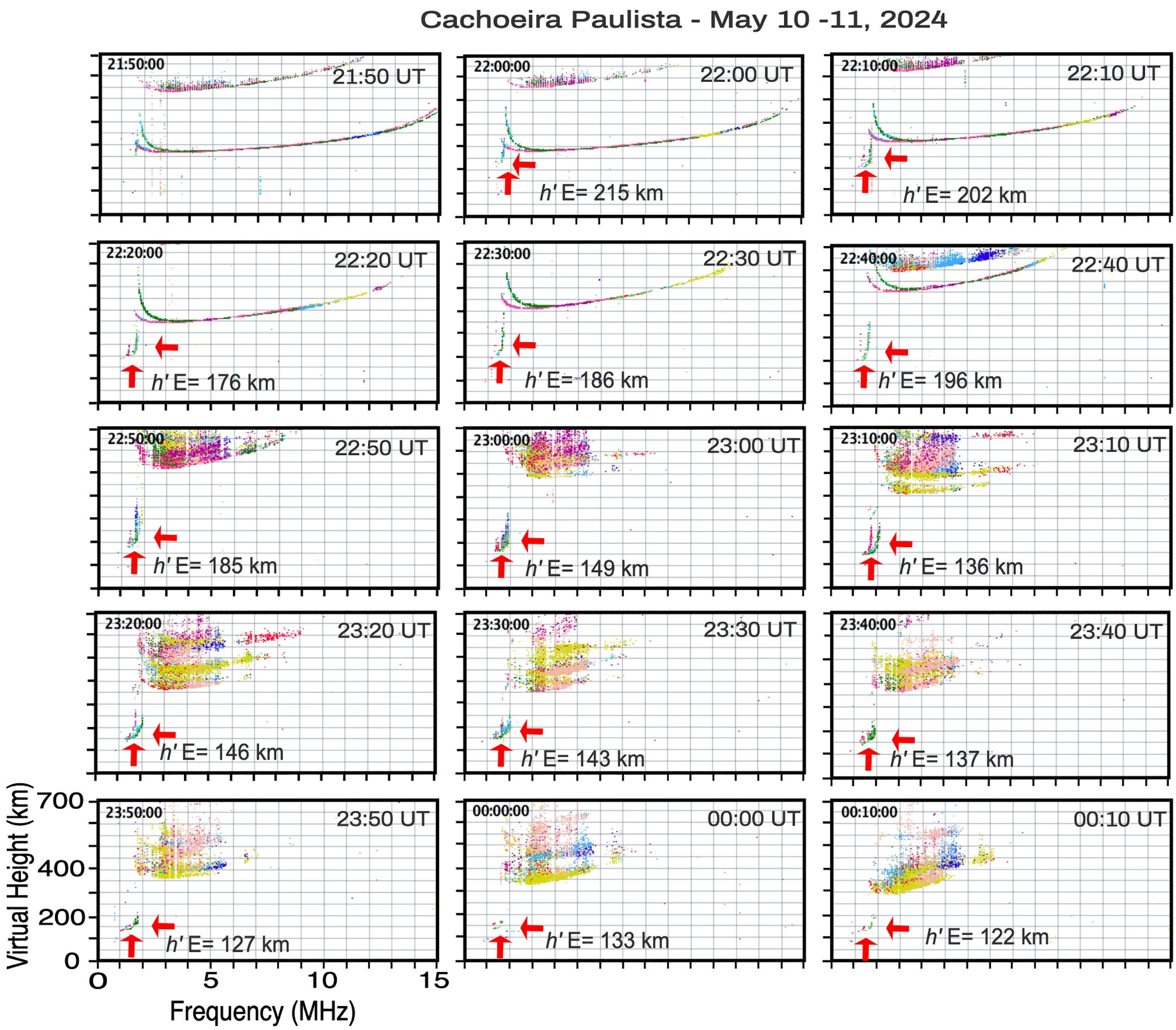

Figure 3. Ionograms at Cachoeira Paulista collected from 21:50 UT on 10 May 2024 until 00:10 UT on 11 May 2024, showing the nocturnal E layer.

processes are much faster than transport terms and, therefore, only depend on the production of ions and their neutralization by loss processes. Thus, there is a maximum ionization around local noon, and its electronic density is significantly reduced at night (Hargreaves, 1992). This implies that equipment that uses the reflection of radio waves in ionized layers, such as Digisondes, does not detect this layer after sunset (Reinisch et al., 2009).

The main indication that an extra ionization occurred in the ionosphere is the presence of the E region during the nighttime in observational data, as seen in Figure 3. This figure shows some selected ionograms between 21:50 UT (18:50 LT (LT = UT-3)) and 00:10 UT (21:10 LT) for CXP on 10–11 May 2024. In this period, as observed in Figure 2d, the magnetic storm was in the main phase. At 21:50 UT, we only observed the F region, which is typical for quiet days. The unusual process started at 22:00 UT when we detected a different layer at high heights around 215 km (*h*'E indicated by the vertical red arrow). The E layer height evolution differs significantly from typical behavior observed during quiet periods (not shown here). By 22:10 UT, this layer is clearly identified as a nighttime E-layer, which exhibited a rapid descent movement from 22:00 UT until 23:10 UT. After this period, the nocturnal E layer experienced a mild oscillation, and the E region establishes in their typical heights (reaching up to a maximum of 150 km) and remained mostly stable, as seen in the ionograms. In contrast, at higher altitudes,

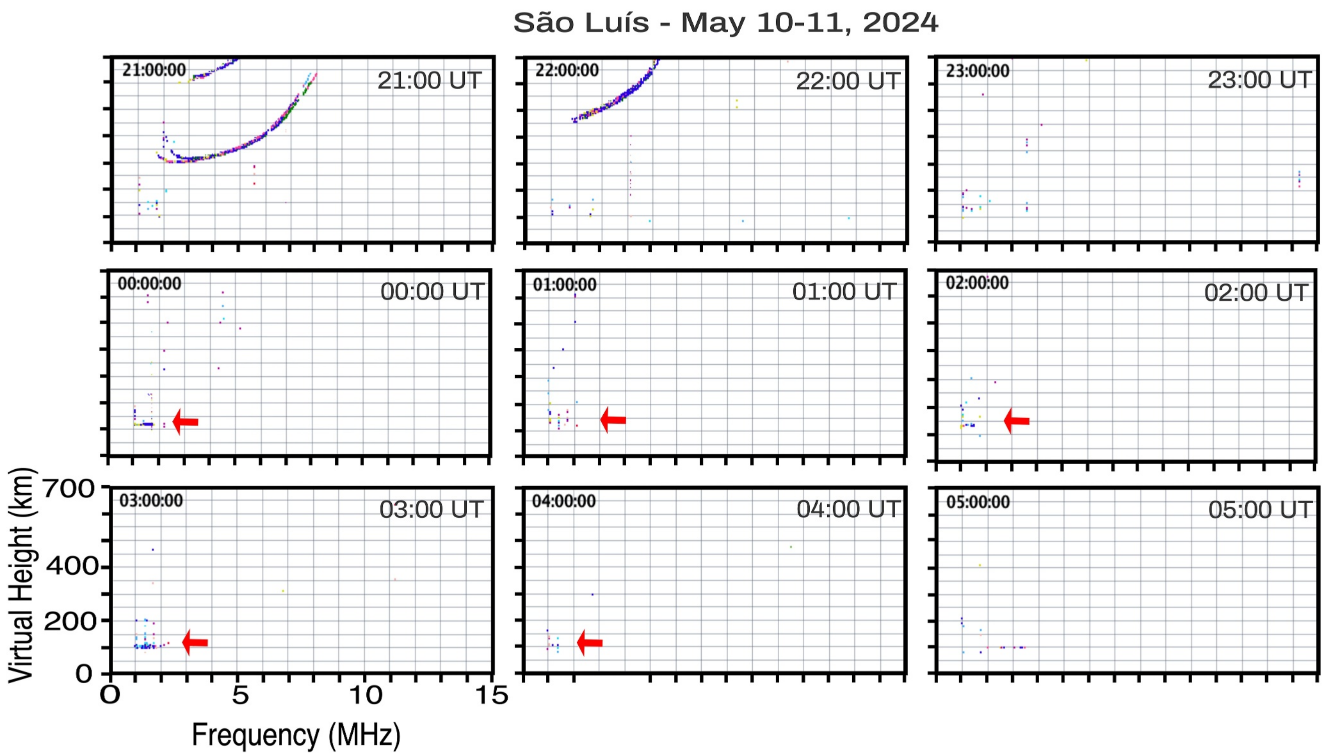

Figure 4. Ionograms over São Luís between 21:00 UT on the 10th and 05:00 UT on the 11th of May 2024, in increments of half an hour, showing the E region at nighttime.

the F region showed an upward drift until 22:50 UT. Therefore, a very interesting point is the unusual opposite movements of the E and F regions. Although the nighttime E region is shown in Figure 3 until 00:10 UT, it lasted until 04:00 UT (01:00 LT).

The nighttime E region also occurred in São Luís (SLZ), a station near of the magnetic equator and further from SAMA, as shown in Figure 1. Figure 4 shows the ionograms between 21:00 UT on the 10th and 05:00 UT on the 11th of May 2024, in increments of an hour. During this time, a weak trace similar to the E region appeared between 01:00 and 04:00 UT (red arrow). At 03:00 UT, the E region was more evident, and the ordinary and extraordinary traces became clearer. In the hours following 05:00 UT, the E layer began to disappear. The F region absence in the ionograms is explained by its rapid rise due to the disturbed eastward penetration electric field since this period is at sunset, which will be discussed after. Thus, an eastward PPEF intensified the pre-reversal enhancement (PRE), raising the F layer and causing the super-fountain effect. Several authors have already studied this fact (Abdu, Kherani, Batista, & Sobral, 2009; Batista et al., 1991), which explains the F-region absence in the ionograms from 23:00 UT.

The primary outcome of this study was the Es_c layer detected in ionograms at nighttime for the first time during this extreme geomagnetic storm. Figure 5 shows the development of the Es_c layer in ionograms over CXP between 01:50 UT (22:50 LT) and 0340 UT (00:40 LT). First, we called attention to a different trace, similar to the Es_c layer, at low frequencies (*fb*Es ~ 2 MHz; *ft*Es ~ 2.5 MHz) and high altitudes (*h'*Es > 180 km). The *ft*Es and *h'*Es are indicated by red arrows in Figure 5. This trace was observed between 01:50 UT and 02:10 UT and can be classified by an "*h*" type for their height localization. Subsequently, this layer exhibited a downward movement, and the Es_c layer is clearly identified at 02:20 UT. At this moment, the Es_c layer settles at heights of 130–140 km until it disappears at 03:30 UT. Notice that the Es layer downward movement is now less abrupt than in earlier instances. The *h'*Es was at 147 km at 02:20 UT and decreased to 137 km by 03:00 UT. The Es layer height evolution is common during daytime as shown in Conceição-Santos et al. (2019), and Moro et al. (2023). The main point here is that this behavior is occurring at nighttime, which has never been observed. In fact, we only detect the Es_f trace at night, as noted in previous climatological studies regarding the Es layer over SAMA stations (e.g., Conceição-Santos et al., 2019; Moro et al., 2023; Resende et al., 2013).

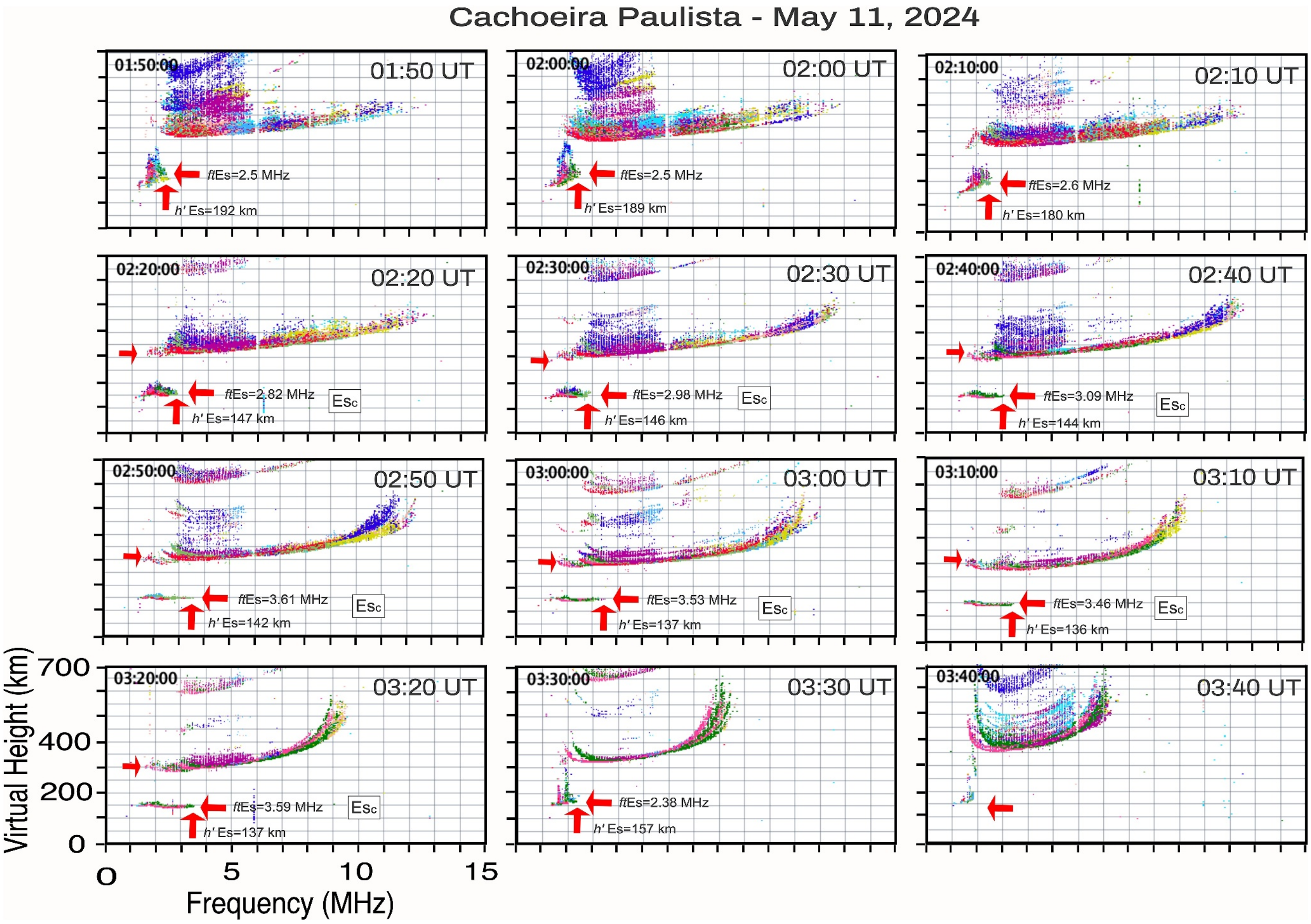

Figure 5. Ionograms over Cachoeira Paulista between 01:50 UT and 03:40 UT on the 11th of May 2024, showing the nighttime Es_c layer.

Finally, we observed another important point here which the trace's second reflection, confirming that it is not an irregular layer. Additionally, we saw that as the Es_c layer becomes evident, the spread F in the F region almost completely disappeared. The spread F was strong again at 0350 UT (not shown here) when the Es_c layer was no longer detected in Digisonde data.

4. Discussion About the Extra Ionization Over the SAMA Region

In this strong magnetic storm, we notice that a convection electric field may be penetrated, as indicated by the sharp increase of Bz and SME index at 2200 UT in Figures 2a and 2c. The eastward PPEF explains the rise of the F region observed in the ionograms over CXP and SLZ (Abdu, 1997; Abdu et al., 2006; Blanc & Richmond, 1980; Fejer, 1997; Fejer et al., 2008). On the other hand, the rapid downward drift of the E region over CXP suggested that there were other effects besides electric fields, such as ambipolar diffusion, and neutral winds. This behavior can be seen in the plasma vertical motion (V_z) expression:

$$V_z = V_D \cos I \pm U_F \cos I \sin I - w_D \sin^2 I, \tag{4}$$

where V_D represents the true vertical drift velocity at the magnetic equator, which is influenced solely by the electric field. In fact, V_D can be estimated using the equation $\frac{dh'F}{dt} - \beta H$ at an equatorial station ($h'F$ is the F region virtual height, β is the recombination coefficient, and H is scale height). Additionally, I is the magnetic inclination angle, U_F is the meridional wind in the F region (positive northward), and w_D is the diffusion term (Nogueira et al., 2011; Resende et al., 2021).

The vertical drift at CXP (V_z) can be seen as the sum of the true vertical drift from the magnetic equator (V_D) and the effects of winds and diffusion. It is important to emphasize that V_D over the equator is only used to estimate the electric field contribution to vertical movement at low latitudes. Thus, Equation 4 demonstrates that the E region downward drift over CXP (between 130 and 215 km, as shown in Figure 3) is influenced by the ambipolar diffusion and winds since this behavior occurs at nighttime and CXP is located further away from the magnetic equator. In other words, we believed that the diffusion and neutral winds were responsible for the observed vertical downward movement in the E region heights.

Santos et al. (2016) investigated the magnetic disturbed days around magnetic storms over the Brazilian and Peruvian sectors. Such work aimed to analyze the change in the zonal drift direction at night (disturbed zonal drift). This process was associated with the entry of energetic electrons in the main phase of the magnetic storm, which occurs concomitant with ring current enhancement, causing an additional ionization and increasing Hall conductivity. This process, in turn, triggers a disturbed drift toward the westward in the nighttime. The details of the study by Santos et al. (2016) are separated from the results presented here. However, the authors showed that an extra ionization process was necessary for the observed phenomena. Previous works such as Abdu et al. (1981, 2005) mentioned that the E region during the nighttime over SAMA regions is convincing evidence for ionization enhancement caused by energetic particle precipitation. These authors evidenced that the nighttime E region presence in ionograms over CXP is associated with the particle precipitation mechanism.

However, the magnetic field is still weaker compared to the rest of the globe (around 25,000 nT- Figure 1). Also, this region is strongly influenced by disturbed electric fields from PPEF (Abdu, 1997) and DDEF (Blanc & Richmond, 1980). During this magnetic storm, several atypical behaviors occurred that are not linked to the purpose of this work. Among them, we can mention the super-fountain effect, in which the F region rose excessively, confirming the eastward penetration electric field, and the plasma diffused through the field lines to higher latitudes (reaching 40° and not shown here) (Balan et al., 2009).

Thus, the E region occurrence over SLZ in atypical hours is another evidence of the additional ionization probably due to the particle precipitation mechanism. Resende et al. (2013) and Denardini et al. (2016) showed a spread trace of the Es layer during recovery magnetic storm phases, and it was associated with electric particle precipitation. They named this trace the auroral Es layer (Es_a layer). Nevertheless, they stated that other studies would be necessary to conclude that particle precipitation would act on the Es layer over regions far from the SAMA center. Recently, Resende et al. (2020) analyzed a strengthened and spreading Es layer over Boa Vista (BV, 2.8°N, 60.7°W, dip ~18°), a low latitude region over the Brazilian sector, which is also far from the SAMA center. They observed this Es layer during the recovery phase of the magnetic storm of 21–22 January 2016. In their conclusion, the authors associated this atypical Es layer with a westward electric field during the disturbance dynamo effect. Resende et al. (2020) discarded the possibility of particle precipitation based on other studies, such as Fürst et al. (2009), Ginet et al. (2007), and Da Silva et al. (2016), who mentioned that regions located in the northwest boundary of the SAMA may not receive significant influence of the electron energetic particles. Abdu et al. (2014) also mentioned that the particle precipitation influence in the equatorial region is due to the E-F region coupling, increasing the Hall and Pedersen conductivities ratio ($\sum H/\sum P$) and modifying the zonal drift velocity. Recently, Resende et al. (2021) analyzed 22 magnetic storms and they did not observe any atypical behavior in the Es layer over CXP. Thus, there is still a discussion about how effective particle precipitation processes are in regions far from the SAMA center.

Two processes explain the entry of energetic particles into SAMA. One is the collisional process by Coulomb scattering in which low-energy particles from the inner radiation belt enter the mirroring points at 100 km (Abdu et al., 1981, 2005). Another process is the interaction of Hiss-type magnetospheric waves with electrons, especially those of low energies (0.5 keV to tens keV), which causes pitch angle scattering, violating the first and/or second adiabatic invariant (Da Silva et al., 2022). This second process is what explains the presence of the Es_a layer in the ionograms in the SAMA region, which has already been studied in the literature (Batista & Abdu, 1977; Da Silva et al., 2022; Moro et al., 2022). The auroral trace or Es_a layer occurs mainly in the recovery phase of the magnetic storm. The previous publications suggested that the reason for the condition to generate the Es_a layer over SAMA is the particle injections from the magnetotail, which are associated with the substorms. In fact, the Es_a layer typically indicates particle precipitation mechanism action. However, we believe that the Es_a layer occurrence relies on a background mechanism that facilitates the formation of typical Es layers, such as types "l" and "f", which are influenced by tidal winds. The tidal wind components were low this month, in which the zonal diurnal tide amplitude usually is around 5–10 m/s in May over CXP (Batista et al. (2004)). Thus, this tidal wind behavior results in weak or absent typical Es layers during the nighttime, the Es_a layer was not observed during this event.

Therefore, our focus in this study is on the main phase of the magnetic storm in which the E region appeared at night, even in regions far from the SAMA center. As the E region was observed at the beginning of the magnetic storm's main phase, we supposed there was an increase in the collisional process due to the particle entry into SAMA.

4.1. The Atypical Es_c Layer Over the SAMA Region

We emphasize here three uncommon dynamical processes that occurred during the Es_c layer development such as (a) the nocturnal Es_c only appeared due to the E layer presence, (b) some intensification oscillation that became the wind shear mechanism effective to allow the Es_c layer formation, and (c) the anti-correlation between spread F and the Es_c layer trace. As discussed in the previous sections and shown by the simulations, we believed that the extra ionization due to the particle precipitation was the explanation for the E region's presence. Once the E region is detected, the Es_c layer can appear since there is a continuous trace of the E region (Piggott & Rawer, 1978).

An interesting fact is related to the Es layer formation on the hours/days before the CME arrived, in which this layer appeared weak with frequencies around 2–4 MHz. Precisely, the Es layers were weak during the daytime on 10 May 2024 (see example of Figure 1b), and it disappeared after the sunset. This behavior is expected since the tidal wind amplitudes are low in May and June, as seen in Batista et al. (2004). During the autumn, the meridional and zonal winds for diurnal and semidiurnal do not reach values more than 30 m/s over Cachoeira Paulista and, consequently, the Es layers are much weaker compared to summer and spring seasons (Resende et al., 2017).

The different types of Es layers are distinguished by their appearance in ionograms, which are linked to the underlying physical mechanisms. Es layers of types "l" and "f," which form at lower altitudes (∼100 km), tend to have longer durations because they are influenced by the zonal component of tidal winds and the significant presence of metallic ions at these altitudes. The meteor ablation and interaction ion-neutral collision has an effectivity around ∼100 km altitude, where the $Es_{f/l}$ layer traces frequently (Haldoupis, 2011). As metallic ions (Fe^+ and Mg^+) have a longer lifetime (Kopp, 1997), the flat and low Es layer types appear in ionograms at all hours of the day.

In contrast, the formation of Es_c and Es_h layers is attributed to the other components of tidal winds, mainly the meridional component. Es_h layers form above 150 km due to semidiurnal meridional tidal winds and display downward movement, which contributes to the development of the Es_c layer. The Es_c layer is primarily influenced by the diurnal components of tidal winds. As their trace is continuous with the E region and acts on molecular ions, the Es_c layer is a daytime phenomenon.

In fact, the Es_c layer has been detected only during the daytime until now. Conceição-Santos et al. (2019) analyzed the different Es layer types over two stations, Jataí (JAT, 17.9°S, 51.7°W, dip ∼13.4°S), and São José dos Campos (SJC, 23.2°S, 45.8°W, dip ∼21.0°S) during the year 2016 by seasons. Such stations are also under the SAMA influence. Their seasonal analysis showed that the flat/low types ($Es_{f/l}$) are the most frequent over both stations than other types (Es_c and Es_h). The authors also observed that the Es_c occurred in the daytime for all seasons analyzed. Additionally, the Es_c layer was more common in the autumn and spring, weakening as winter approached. The same result was observed in a recent statistical study by Moro et al. (2023) over Santa Maria (SMS, 29.7°S, 53.8°W, dip ∼37°S), a station in the SAMA's center. The Es_c layer over the SMS was detected exclusively during the daytime from July 2019 to June 2020. Moro et al. (2023) separated their results into seasons, and the Es_c appeared mainly in the spring and summer. The authors proposed that the Es_c layer only developed during the daytime because of higher ionization. In other words, the Es layer types formed above 120 km, such as "*c*" and "*h*", would have their composition by molecular ions while the Es layers located in lower altitudes would be produced by the metallic ions.

The Es_c layer occurrence in this study was another verification that the extra ions were present during this geomagnetic storm event. Since the winds are weak in this period and the Es_c layer is only observed in the daytime, other physical mechanisms had to act to explain the presence of this specific layer. Analyzing the entire scenario already discussed here, a proposal would be that the entry of particles over the SAMA may have generated oscillations in the atmosphere. Indeed, a new oscillation over short periods (∼2 hr) may have been

10.1029/2024JA033167

triggered by Joule heating when particles precipitated in the ionosphere's height, resembling the auroral zones (Guo et al., 2015). As this layer is located above 130 km, it is believed that this oscillation may have been generated in situ. The abrupt descent movement between the times of 02:10 UT and 02:20 UT can be attributed to the westward penetrating electric field as indicated by the F layer downward drift in Figure 7.

Lal (2006) found that severe geomagnetic storms influence the tropospheric acoustic gravity waves at equatorial and low latitude stations over the Indian sector due to the density variation in the atmosphere. Another work done by Mandal and Pallamraju (2020) in low latitudes over the Indian sector shows that the redistribution of energy and momentum in the Earth's atmosphere during magnetic storms induced oscillations with a period of 1–2 hr. In such work, the authors emphasized a correlation between the oscillations defined as gravity waves of the short period and the intensification of the AE index. Hence, even in regions far from the auroral zones, oscillations may occur due to the heating of the atmosphere as a whole. Thus, the entry of particles during this intense magnetic storm that occurred on 10–11 May 2024, can have intensified these oscillations, making the wind shear mechanism effective and explaining the nighttime Es_c layer presence over the SAMA. The Es_c layer was probably formed by the new molecular ions (N_2^+ and O_2^+) since it had little durability, lasting a few hours (∼2 hr).

Unfortunately, we do not have data that can confirm the existence of these fluctuations in the heights of E region. However, as already analyzed in some studies, it is possible to infer the existence of short-period oscillations and gravity waves using Digisonde data around the absolute heights above 170 km (Abdu, Kherani, Batista, De Paula et al., 2009; Abdu et al., 1982). As the Es_c layer starts to appear at high heights (h'Es = 179 km), we examined the wave fluctuations in electron density immediately preceding their development. Thus, the true heights in ionograms (hF) were also used to extract the wave oscillations over CXP, as shown in Figure 6. The color lines represent the specific plasma frequencies at 2 MHz (red), 3 MHz (blue), 4 MHz (pink), and 5 MHz (green) between 22:00 UT and 04:00 UT on 10–11 May 2024. Notice that we had the manifestation of the wave oscillation in some hours (gray dashed lines), which has a downward phase propagation. We draw attention to the period just before 02:00 UT, where the data show an apparent oscillation in low frequencies. Soon after this oscillation, a new layer located at almost 190 km was observed as seen in Figure 5 (indicated by the orange arrow in Figure 6). Thus, a possibility is that an in-situ oscillation may have arisen in the neutral atmosphere due to Joule heating caused by the entry of particles into the SAMA region, as occurs in auroral sites.

Although it is not the scope of this work, it is important to mention that during sunset times, there was an abrupt upward drift in the F layer over the equatorial region of São Luís due to the eastward penetration of the electric field, which led to the emergence of plasma bubbles, reaching the low latitude regions since they are aligned with the magnetic field. For this reason, the spread F was observed in CXP, even being a period (month of May) when plasma bubbles are typically weaker and confined to equatorial regions (Abdu et al., 1985). However, it was observed that when the Es_c layer trace appeared clearly (at 02:10 UT), the spread F started to weaken (Figure 5) over CXP. The Es_c layer and the absence of the spread F happened together, and it lasted until 03:30 UT. At 03:40 UT, the Es_c layer disappears completely, and the spread F is observed in ionograms again. Therefore, the observational data showed an anti-correlation of these two phenomena: the Es layer and the spread F associated with the plasma bubbles.

The explanation of the relationship between the development of equatorial spread F and the Es layer at low latitudes is under discussion. Stephan et al. (2002) analyzed this relationship, calculating the modifications in the integrated Pedersen conductivity in the flux tube for E and F regions ($\sum_P E, \sum_P F$) during the sunset hours that affected the growth rate of the Rayleigh-Taylor instability (γ_{RT}), responsible for the plasma bubbles development. In other words, the authors explained that with a strong Es layer present at sunset times, there would be a significant increase in the integrated Pedersen conductivity, which would inhibit the appearance of irregularities in the F region. This statement becomes clear to understand when we see how the bubble growth rate (γ_{RT}) behaves (Haerendel & Eccles, 1992):

$$\gamma_{RT} = \frac{\sum_P F}{\sum_P^N E + \sum_P F + \sum_P^S E}\left(V_D - U_F - \frac{g}{\nu_{in}}\right)\frac{\nabla n}{n} - R, \tag{5}$$

in which g is gravitational acceleration, ν_{in} refers to the ion-neutral collision frequency, n is the electron density, and R is the chemical recombination rate. As mentioned before, V_D is the vertical plasma drift and U_F is the conductivity-weighted flux tube integrated vertical wind. Equation 5 provides the necessary ingredients for the

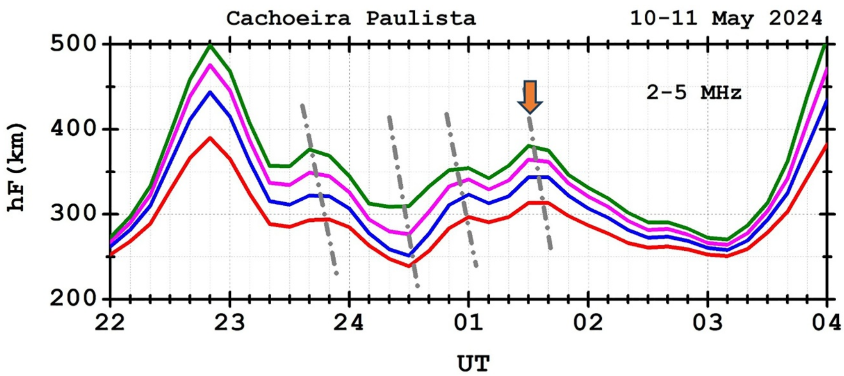

Figure 6. The F layer true heights (*h*F) at plasma frequencies 2 MHz (red), 3 MHz (blue), 4 MHz (pink), and 5 MHz (green) between 22:00 UT and 04:00 UT on 10–11 May 2024. The gray dashed lines represent the wave oscillation and orange arrow the Esc layer occurrence.

irregularities' occurrences in the equatorial regions. Generally, the preliminary condition is well-known, and it occurs during the pre-reversal enhancement of the zonal electric field (PRE) (Abdu, Kherani, Batista, & Sobral, 2009; Fejer et al., 2008), in which the ν_{in} and R are low when the F region uplifts. The PRE is a consequence of the E and F regions uncoupling in the post-sunset hours since the E region conductivity decays significantly. However, a strong Es layer presence in such hours could lead to significant suppression of the γ_{RT} due to the conductivity increase. In the study of Stephan et al. (2002), the cases occurred in quiet and disturbed periods.

Recently, the connection between the spread of F and Es layers was verified by Singh and Sripathi (2020) over two coupling Indian stations, one located over the equatorial region and another at low latitude. These authors performed their study during the magnetic storm occurrences in 2007–2015. Their observations and conclusions are similar to the work of Stephan et al. (2002) for post-sunset hours, which emphasizes that the strong Es layer presence caused the decrease of PRE due to modifications in the field-line-integrated Pedersen conductivity, affecting the plasma bubbles development. However, Singh and Sripathi (2020) advanced further in their analysis. They showed that it is possible that a relationship between the Es layers and the development of plasma bubbles also occurs in the hours after sunset. In other words, these two phenomena would have a nightly correlation or anti-correlation. They credited their results to the disturbed electric fields that Resende et al. (2020, 2021) later verified in the literature for Brazilian regions. The effect of the electric fields would reach the E and F regions separately and not in a coupled process.

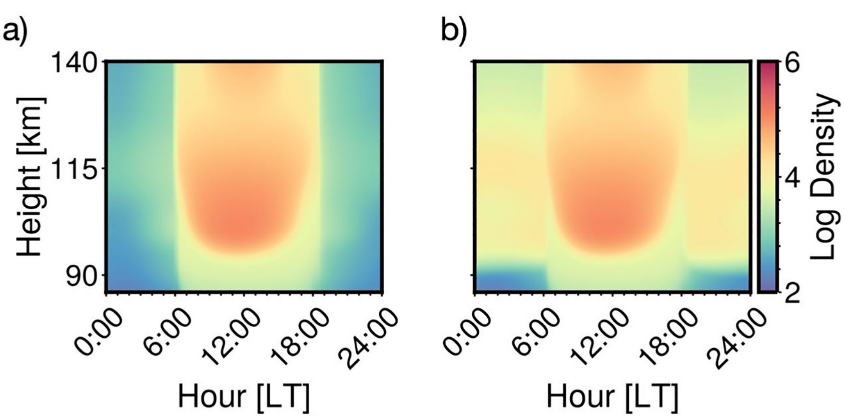

Figure 7. Electron density in log scale (electrons/cm^3) as a function of Local Time and height (km) simulated by MIRE considering (a) without particle precipitation, and (b) include the same extra particle precipitation flux given in Fang et al. (2010).

The effect of the energetic particle precipitation became evident once the E region was formed. Thus, there was again a coupling between the E and F regions as if it was daytime. At this time, the increase in Hall conductivity ($\sum$H) connects the circuit between these ionospheric regions again, as Abdu et al. (2013) mentioned. However, even with an increase in conductivity, the spread F did not disappear. The inhibition of spread F only occurred when there was an Es (Es_c) layer, showing that an increase in conductivity high enough was needed to cause irregularity suppression (Singh & Sripathi, 2020). Furthermore, it was seen that the F layer tended to descend during the spread F absence, which may be due to the westward disturbed zonal electric field. The disturbed electric field could also inhibit the irregularity in the F region. Nevertheless, soon after the Es_c layer disappears, the F spread returns, which indicates that the disturbed electric field processes may be secondary. Therefore, it is possible that to exist an anti-correlation of these two phenomena, there must be a threshold of increase in conductivity in the E region that overcomes the effect of the zonal electric field penetration. The value threshold will be investigated in future works.

4.2. Modeling the Nighttime E Layer Due To Particle Precipitation

Abdu et al. (2005) analyzed the E region heights during the quiet times, and they showed that there is a higher background electronic density in SAMA compared to regions outside it. They used the *ft*Es parameter of the Es layer because ionosondes cannot detect the E region during these times, as we mentioned before. The authors concluded that the collisional interaction between the low-energy electrons and the neutral atmosphere is continuous since the inner radiation belt reached ∼100 km over the SAMA. During the disturbed period, the nocturnal E region can appear in ionograms, as seen in Abdu et al. (2013). When this behavior occurs, the authors concluded that it is a great indication of particle precipitation mechanism acting in the ionosphere. To quantify this behavior, we used the simulations obtained from MIRE, which successfully simulates the E region and Es layer considering the chemistry processes, winds, and electric fields, as mentioned in Resende et al. (2017, 2020, 2021) and Moro et al. (2022).

Figure 7a presents the Height-Time Map (HT) of the E region electron density profile, as simulated by MIRE (color scale) over CXP on 11 May 2024. Figure 7b, on the other hand, depict the same profile but simulate that extra ionization, including the flux given in Fang et al. (2010), which best matches the reference model found in the literature. Here, we propose that the nighttime E region was formed due to an extra ionization driven by electron particle precipitation over the SAMA region. We included the particle precipitation flux (Equation 3) in MIRE for the first time to verify the nighttime behavior around 100–140 km. The purpose is to examine the extent of low-energy electron flux entering the atmosphere and how it could intensify the E region to the level detected by Digisonde.

This simulation that excludes the extra ionization at nighttime caused by the particle precipitation, show a typical behavior that is a high E region density in the daytime (06:00–18:00 LT) and low nocturnal values. As seen in Figure 7a, the maximum ionization is around $10^{5.5}$ electrons/cm^3 12:00 LT. In nighttime, the values do not exceed 10^3 electrons/cm^3. When we included a precipitation flux in MIRE using $Q_o = 1$ erg (Figure 7b), one can see that there is an increase in the E-region electronic density at night hours. The E region electron density became 10^4 electrons/cm^3 in that case.

To see the exact particle precipitation flux in the ionosphere during this magnetic storm, we fit the different scenarios in the simulations. Thus, we could match the observational data driven by Digisonde and MIRE simulations by increasing the extra ionization (Q_o). Figure 8 compares the E region electron density (n_e) using the relationship $n_e = 1,24x10^4\left(foE^2\right)$ to provide better insight into the particle precipitation effect in the ionosphere during the disturbed times (gray line). The *fo*E refers to the critical frequency of the E region given in MHz, and the final result is given in the log scale from 1900 LT to 0400 LT. Notice that the E region reached values higher than $10^{4.5}$ electrons/cm^3. The blue and red lines are the MIRE simulations considering only the typical chemistry processes and the particle precipitation with $Q_o = 1$ erg, respectively. It is clear that the enhancement of the particle precipitation total energy needs to be more intense than the reference to represent the observational data obtained during the magnetic storm adequately.

Therefore, the best acceptable result found in our simulation was 10 times more than the reference flux in Fang et al. (2010), that is, by selecting $Q_o = 10$ erg, showing in the orange line of Figure 8. In this case, the density reached $10^{4.6}$ electrons/cm^3, agreeing with the electronic density driven by the *fo*E values. This behavior showed

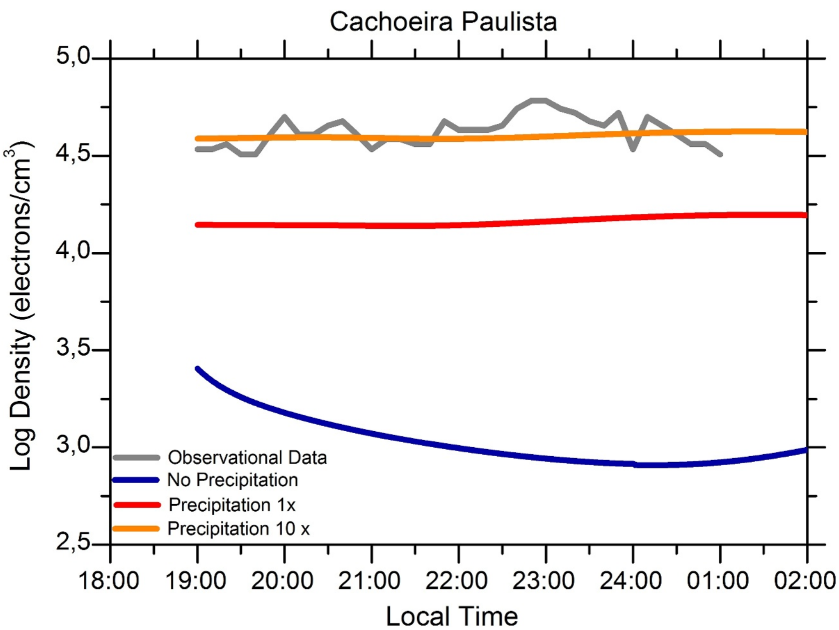

Figure 8. The comparison between the electron density of the E region (log scale) between observational data (gray line), and simulation of MIRE. Blue line refers the simulation with no particle precipitation inclusion, red line refers the particle precipitation with the parametrization Q_o, and orange line the particle precipitation with the parametrization 10 Q_o.

that this geomagnetic storm event was very intense and uncommon, and it was capable to modify all the ionosphere over the SAMA. In fact, the simulations showed an interesting aspect that the ionosphere behaves as if it were daytime, resulting in several phenomena that are atypical for nighttime hours.

The E region presence became possible detected the nighttime presence of a sporadic cusp-type layer (Es_c), which, to the best of our knowledge, has not been previously documented in the literature. In our study, the process was more complex due to the presence of SAMA. All phenomena occurred together, such as the entry of particles into a region with a weaker magnetic field, disturbed electric fields influencing the rise and fall of the ionospheric layers (E and F regions), the emergence of short-period oscillations densifying a new layer (Es_c layer), and the weakening of the spread-F during the occurrence of Es_c layer.

Finally, our study indicates that energetic particles may be entering the atmosphere due to collisional processes by Coulomb scattering. Thus, the low-energy electrons entered the SAMA atmosphere at the lower mirror point of 100 km, which is lower compared to other stations. This process is continuous, occurring even during quiet periods. However, it is believed that there was a sudden intensification due to the very intense magnetic storm, affecting sectors such as SLZ. Thus, the additional number of charged particles ionized the elements in the E region, primarily forming NO^+ and $O_2{}^+$. Consequently, this layer was detected by the Digisonde, providing strong evidence of particle precipitation.

5. Conclusions

This study evaluated a peculiar behavior in the nighttime lower ionosphere over CXP, a low-latitude station located inside SAMA. The E region and Esc layer appear during the main phase of the strong magnetic storm that occurred on 10–11 May 2024 (SYM-H < -500 nT). We analyzed the Digisonde data and performed simulations to understand the dynamic processes of this atypical Es layer formation.

We observe a nocturnal E region in Digisonde data between 21:50 UT (18:50 LT (LT = UT-3)) and 00:10 UT (21:10 LT) for CXP on 10–11 May 2024, that is an indication of the extra ionization caused by particle precipitation. The nighttime E layer performed a quick decedent movement under the influences of disturbed neutral wind and ambipolar diffusion which was responsible for the downward motion. Furthermore, we observe the E region at SLZ, a region far from the SAMA region's center. The additional ionization over CXP and SLZ that probably caused the E region is evidence of the particle precipitation mechanism.

To confirm our hypothesis about the particle precipitation, we included for the first time the flux of energetic electrons in MIRE based on Fang et al. (2010). We analyzed the variation of the E region electron density in different scenarios. The first simulation referred to the typical profile of the E region, which showed a maximum ionization of 10^3 electrons/cm^3 at night. When we added a precipitation flux with the reference value in Fang et al. (2010) ($Q_o = 1$ erg $= 6.242 \times 10^{11}$ eV), we observed an increase in the E region electronic density at night hours around 10^4 electrons/cm^3. However, we verified that an additional ionization increases of around 10 times more that reference value is needed so that the simulation results match the observational data (*fo*E).

Two processes explain the entry of energetic particles into SAMA. One is the collisional process by Coulomb scattering in which low-energy particles from the inner belt enter the mirroring points at 100 km. Another process is the interaction of Hiss-type magnetospheric waves with electrons, especially those of low energies (0.5 keV to tens keV), which causes pitch angle scattering, violating the first and/or second adiabatic invariant. Based on the MIRE simulations, we believed that the entry of particles was due to the mirroring point on the SAMA at a lower height (collisional process), allowing the interaction with the neutral atmosphere, forming the E region. The fact that the E region was present means that the ionosphere behaved as if it was daytime, resulting in several phenomena that are atypical for nighttime hours.

The main result in the E region heights in this study was the Es_c layer presence at nighttime never seen before in Digisonde data. The Es_c nocturnal development occurred due to the E layer presence. Here, we suggest a new oscillation over short periods (~2 hr) that Joule heating may have triggered when particles precipitated in the ionosphere's height, resembling the auroral zones. As this layer is located above 130 km, it is believed that this oscillation may have been generated in situ. We showed that short-period oscillations, in which the wind shear mechanism could be effective, create a new layer. Furthermore, we observed an anti-correlation between spread F and the Es_c layer trace that was associated with an increase in the E region conductivity, causing a suppression of the irregularity.

Finally, the combined results from the model and observational data had the potential to significantly advance our understanding of the particle precipitation effect over the SAMA region, and the physical mechanism that can be affected during this strong space weather event. This research could have a profound impact on our ability to predict and mitigate the effects of such events, making it a crucial area of study for the future.

Data Availability Statement

The Digisonde data from Cachoeira Paulista and São Luís can be downloaded upon registration at the Embrace webpage from INPE Space Weather Program in the following link: http://www2.inpe.br/climaespacial/portal/en/. The interplanetary medium conditions at the L1 Lagrangian point were obtained from OMNIWeb database in https://omniweb.gsfc.nasa.gov/index.html. The magnetic indices SME and SYM-H are available in https://supermag.jhuapl.edu/indices and https://wdc.kugi.kyoto-u.ac.jp, respectively.

Acknowledgments

L. C. A. Resende would like to thank the China-Brazil Joint Laboratory for Space Weather (CBJLSW), National Space Science Center (NSSC), Chinese Academy of Sciences (CAS) for supporting her postdoctoral This work was supported by the International Partnership Program of Chinese Academy of Sciences, Grants 183311KYSB20200003 and 183311KYSB20200017. C. M. Denardini thanks CNPq/MCTI, Grant 302675/2021-3. J. Moro, A. M. Santos, V. F. Andrioli, and L. A. Da Silva thanks the CBJLSW/NSSC/CAS. C. Arras acknowledged the support by Deutsche Forschungsgemeinschaft (DFG) under grant WI 2634/19-1. S S. Chen thanks to CNPq/MCTI (Grants 301449/2024-4 and 172834/2023-6). The authors thank Embrace/INPE for providing Digisonde data, OMNIWeb for providing the interplanetary medium data at L1 Lagrangian point, and SuperMAG and WDC Kyoto for providing the magnetic indices SME and SYM-H, respectively.

References

Abdu, M., Sobral, J., Nelson, O., & Batista, I. (1985). Solar cycle related range type spread-F occurrence characteristics over equatorial and low latitude stations in Brazil. *Journal of Atmospheric and Terrestrial Physics*, *47*(8-10), 901–905. https://doi.org/10.1016/0021-9169(85)90065-0

Abdu, M. A. (1997). Major phenomena of the equatorial ionosphere-thermosphere system under disturbed conditions. *Journal of Atmospheric and Terrestrial Physics*, *59*(13), 1505–1519. https://doi.org/10.1016/S1364-6826(96)00152-6

Abdu, M. A., Ananthakrishnan, S., Coutinho, E. F., Krishnan, B. A., & Reis, E. M. D. S. (1973). Azimuthal drift and precipitation of electrons into the South Atlantic geomagnetic anomaly during an SC magnetic storm. *Journal of Geophysical Research*, *78*(25), 5830–5836. https://doi.org/10.1029/JA078i025p05830

Abdu, M. A., Batista, I. S., Carrasco, A. J., & Brum, C. G. M. (2005). South Atlantic magnetic anomaly ionization: A review and a new focus on electrodynamic effects in the equatorial ionosphere. *Journal of Atmospheric and Solar-Terrestrial Physics*, *67*(17–18), 1643–1657. https://doi.org/10.1016/j.jastp.2005.01.014

Abdu, M. A., Batista, I. S., Kantor, I. J., & Sobral, J. H. A. (1982). Gravity wave induced ionization layers in the night F-region at low latitudes. *Journal of Atmospheric and Terrestrial Physics*, *44*(9), 759–767. https://doi.org/10.1016/0021-9169(82)90004-6

Abdu, M. A., Batista, I. S., Piazza, L. R., & Massambani, O. (1981). Magnetic storm associated enhanced particle precipitation in the South Atlantic Anomaly evidence from VLF phase measurements. *Journal of Geophysical Research*, *86*(A9), 7533–7542. https://doi.org/10.1029/JA086iA09p07533

Abdu, M. A., de Souza, J. R., Batista, I. S., Santos, M. A., Sobral, J. H. A., Rastogi, R. G., & Chandra, H. (2014). The role of electric fields in sporadic E layer formation over low latitudes under quiet and magnetic storm conditions. *Journal of Atmospheric and Terrestrial Physics*, *115*, 95–105. https://doi.org/10.1016/j.jastp.2013.12.003

Abdu, M. A., Kherani, E. A., Batista, I. S., De Paula, E., Fritts, D., & Sobral, J. H. A. (2009). Gravity wave initiation of equatorial spread F/plasma bubble irregularities based on observational data from the SpreadFEx campaign. *Annales Geophysicae*, *27*(7), 2607–2622. https://doi.org/10.5194/angeo-27-2607-2009

Abdu, M. A., Kherani, E. A., Batista, I. S., & Sobral, J. H. A. (2009). Equatorial evening prereversal vertical drift and spread F suppression by disturbance penetration electric fields. *Geophysical Research Letters*, *36*(19), L19103. https://doi.org/10.1029/2009GL039919

Abdu, M. A., Souza, J. R., Batista, I. S., Fejer, B. G., & Sobral, J. H. A. (2013). Sporadic E layer development and disruption at low latitudes by prompt penetration electric fields during magnetic storms. *Journal of Geophysical Research: Space Physics*, *118*(5), 2639–2647. https://doi.org/10.1002/jgra.50271

Abdu, M. A., Souza, J. R., Sobral, J. H. A., & Batista, I. S. (2006). Magnetic storm associated disturbance dynamo effects in the low and equatorial latitude ionosphere, in Recurrent Magnetic Storms: Corotating Solar Wind Streams. *Geophysical Monograph Series*, *167*, 283–304. https://doi.org/10.1029/167GM22

Arras, C., Wickert, J., Beyerle, G., Heise, S., Schmidt, T., & Jacobi, C. (2008). A global climatology of ionospheric irregularities derived from GPS radio occultation. *Geophysical Research Letters*, *35*(14), L14809. https://doi.org/10.1029/2008GL034158

Balan, N., Alleyne, H., Walker, S., Reme, H., McCrea, I., & Aylward, A. (2008). Magnetosphere-ionosphere coupling during the CME events of 07–12 November 2004. *Journal of Atmospheric and Terrestrial Physics*, *70*(17), 2101–2111. https://doi.org/10.1016/j.jastp.2008.03.015

Balan, N., Shiokawa, K., Otsuka, Y., Watanabe, S., & Bailey, G. J. (2009). Super plasma fountain and equatorial ionization anomaly during penetration electric field. *Journal of Geophysical Research*, *114*(A3), A03310. https://doi.org/10.1029/2008JA013768

Batista, I. S., & Abdu, M. A. (1977). Magnetic storm associated delayed sporadic enhancements in the Brazilian Geomagnetic Anomaly. *Journal of Geophysical Research*, *82*(29), 4777–4783. https://doi.org/10.1029/JA082i029p04777

Batista, I. S., De Paula, E. R., Abdu, M. A., Trivedi, N. B., & Greenspan, M. E. (1991). Ionospheric effects of the March 13, 1989, magnetic storm at low and equatorial latitudes. *Journal of Geophysical Research*, *96*(A8), 13943–13952. https://doi.org/10.1029/91JA01263

Batista, P. P., Clemesha, B. R., Tokumoto, A. S., & Lima, L. (2004). Structure of the mean winds and tides in the meteor region over Cachoeira Paulista, Brazil (22.7°S, 45°W) and its comparison with models. *Journal of Atmospheric and Solar-Terrestrial Physics*, *66*(6–9), 623–636. https://doi.org/10.1016/j.jastp.2004.01.014

Blanc, M., & Richmond, A. D. (1980). The ionospheric disturbance dynamo. *Journal of Geophysical Research*, *85*(A4), 1669–1686. https://doi.org/10.1029/JA085iA04p01669

Carrasco, A. J., Batista, I. S., & Abdu, M. A. (2007). Simulation of the sporadic E layer response to pre-reversal associated evening vertical electric field enhancement near dip equator. *Journal of Geophysical Research*, *112*(A06), 324–335. https://doi.org/10.1029/2006JA012143

Christakis, N., Haldoupis, C., Zhou, Q., & Meek, C. (2009). Seasonal variability and descent of mid-latitude sporadic E layers at Arecibo. *Annales Geophysicae*, *27*(3), 923–931. https://doi.org/10.5194/angeo-27-923-2009

Conceição-Santos, F., Muella, M. T. A. H., Resende, L. C. A., Fagundes, P. R., Andrioli, V. F., Batista, P. P., et al. (2019). Occurrence and modeling examination of sporadic-E layers in the region of the South America (Atlantic) magnetic anomaly. *Journal of Geophysical Research: Space Physics*, *124*(11), 9676–9694. https://doi.org/10.1029/2018JA026397

Da Silva, L. A., Satyamurty, P., Alves, L. R., Souza, V. M., Jauer, P. R., Silveira, M. V. D., et al. (2016). Comparison of geophysical patterns in the southern hemisphere mid-latitude region. *Advances in Space Research*, *58*(10), 2090–2103. https://doi.org/10.1016/j.asr.2016.04.003

Da Silva, L. A., Shi, J., Resende, L. C. A., Agapitov, O. V., Alves, L. R., Batista, I. S., et al. (2022). The role of the inner radiation belt dynamic in the generation of auroral-type sporadic E-layers over South American Magnetic Anomaly (SAMA). *Frontiers*, *9*. https://doi.org/10.3389/fspas.2022.970308

Denardini, C. M., Resende, L. C. A., Moro, J., & Chen, S. S. (2016). Occurrence of the blanketing sporadic E layer during the recovery phase of the October 2003 superstorm. *Earth Planets and Space*, *68*(1), 80. https://doi.org/10.1186/s40623-016-0456-7

Fang, X., Randall, C., Lummerzheim, D., Wang, W., Lu, G., Solomon, S., & Frahm, R. (2010). Parameterization of monoenergetic electron impact ionization. *Geophysical Research Letters*, *37*(22), 22106. https://doi.org/10.1029/2010GL045406

Fejer, B. G. (1997). The electrodynamics of the low-latitude ionosphere: Recent results and future challenges. *Journal of Atmospheric and Terrestrial Physics*, *59*(13), 1465–1482. https://doi.org/10.1016/S1364-6826(96)00149-6

Fejer, B. G., Jensen, J. W., & Su, S. Y. (2008). Seasonal and longitudinal dependence of equatorial disturbance vertical plasma drifts. *Geophysical Research Letters*, *35*, L20106. https://doi.org/10.1029/L035584

Fürst, F., Wilms, J., Rothschild, R. E., Pottschmidt, K., Smith, D. M., & Lingenfelter, R. (2009). Temporal variations of strength and location of the South Atlantic Anomaly as measured by RXTE. *Earth and Planetary Science Letters*, *281*(3–4), 125–133. https://doi.org/10.1016/j.epsl.2009.02.004

Ginet, G. P., Madden, D., Dichter, B. K., & Brautigam, G. D. H. (2007). Energetic proton maps for the South Atlantic anomaly. In *IEEE radiation effects data workshop, Honolulu, HI, USA, 23–27 July 2007* (pp. 1–8).

Gonzalez, W. D., Joselyn, J. A., Kamide, Y., Kroehl, H. W., Rostoker, G., Tsurutani, B. T., & Vasyliunas, V. M. (1994). What is a magnetic storm? *Journal of Geophysical Research*, *99*(A4), 5771–5792. https://doi.org/10.1029/93JA02867

Guo, J., Forbes, J. M., Wei, F., Feng, X., Liu, H., Wan, W., et al. (2015). Observations of a large-scale gravity wave propagating over an extremely large horizontal distance in the thermosphere. *Geophysical Research Letters*, *42*(16), 6560–6565. https://doi.org/10.1002/2015GL065671

Haerendel, G., & Eccles, J. V. (1992). The role of the equatorial electrojet in the evening ionosphere. *Journal of Geophysical Research*, *97*(A2), 1181–1192. https://doi.org/10.1029/91JA02227

Haldoupis, C. (2011). A tutorial review on Sporadic E layers, Aeronomy of the Earth's Atmosphere-Ionosphere. *IAGA Book Series*, *29*(2), 381–394. https://doi.org/10.1007/978-94-007-0326-1_29

Hargreaves, J. K. (1992). *The solar-terrestrial environment: An introduction to geospace - The science of the terrestrial upper atmosphere, ionosphere, and magnetosphere*. Cambridge University Press. https://doi.org/10.1017/CBO9780511628924

Kikuchi, T. (2005). Transmission line model for driving plasma convection in the inner magnetosphere. *Space Plasma Physics*, *155*, 173–179. https://doi.org/10.1029/155GM20

Kopp, E. (1997). On the abundance of metal ions in the lower ionosphere. *Journal of Geophysical Research*, *102*(A5), 9667–9674. https://doi.org/10.1029/97JA00384

Lal, M. (2006). Study of geomagnetic storm induced acoustic gravity waves over equatorial latitude. *Indian Journal of Radio and Space Physics*, *35*, 174–180.

Mandal, S., & Pallamraju, D. (2020). Thermospheric gravity wave characteristics in the daytime over low-latitudes during geomagnetic quiet and disturbed conditions. *Journal of Atmospheric and Solar-Terrestrial Physics*, *211*, 105470. https://doi.org/10.1016/j.jastp.2020.105470

Mathews, J. D. (1998). Sporadic E: Current views and recent progress. *Journal of Atmospheric and Terrestrial Physics*, *60*(4), 413–435. https://doi.org/10.1016/S1364-6826(97)00043-6

Moro, J., Denardini, C. M., Abdu, M. A., Correia, E., Schuch, N. J., & Makita, K. (2012). Latitudinal dependence of cosmic noise absorption in the ionosphere over the SAMA region during the September 2008 magnetic storm. *Journal of Geophysical Research*, *117*(A6), 1–7. https://doi.org/10.1029/2011JA017405

Moro, J., Xu, J., Bageston, J. V., Denardini, C. M., Andrioli, V. F., Resende, L. C. A., et al. (2023). Analysis of blanketing sporadic-E layer and associated tidal periodicities over a Brazilian station undergoing a transition from low latitude to midlatitude. *Journal of Geophysical Research: Space Physics*, *128*(12), e2023JA031947. https://doi.org/10.1029/2023JA031947

Moro, J., Xu, J., Denardini, C. M., Resende, L. C. A., Da Silva, L. A., Chen, S. S., et al. (2022). Different sporadic-E (Es) layer types development during the August 2018 geomagnetic storm: Evidence of auroral type (Esa) over the SAMA region. *Journal of Geophysical Research: Space Physics*, *127*(2), e2021JA029701. https://doi.org/10.1029/2021JA029701

Nogueira, P. A. B., Abdu, M. A., Batista, I. S., & Siqueira, P. M. (2011). Equatorial ionization anomaly and thermospheric meridional winds during two major storms over Brazilian low latitudes. *Journal of Atmospheric and Solar-Terrestrial Physics*, *73*(11–12), 1535–1543. https://doi.org/10.1016/j.jastp.2011.02.008

Piggott, W. R., & Rawer, K. (1978). *U.R.S.I. handbook of ionogram interpretation and reduction (23A)* (p. 146). World Data Center A for Solar-Terrestrial Physics, NOAA. Retrieved from https://repository.library.noaa.gov/view/noaa/10404

Reinisch, B. W., Galkin, I. A., Khmyrov, G. M., Kozlov, A. V., Bibl, K., Lisysyan, I. A., et al. (2009). The new Digisonde for research and monitoring applications. *Radio Science*, *44*(1), RS0A24. https://doi.org/10.1029/2008RS004115

Resende, L. C. A., Batista, I. S., Denardini, C. M., Batista, P. P., Carrasco, A. J., Andrioli, V. F., & Moro, J. (2017). Simulations of blanketing sporadic E-layer over the Brazilian sector driven by tidal winds. *Journal of Atmospheric and Solar-Terrestrial Physics*, *154*, 104–114. https://doi.org/10.1016/j.jastp.2016.12.012

Resende, L. C. A., Denardini, C. M., & Batista, I. S. (2013). Abnormal *fb*Es enhancements in equatorial Es layers during magnetic storms of solar cycle 23. *Journal of Atmospheric and Solar-Terrestrial Physics*, *102*, 228–234. https://doi.org/10.1016/j.jastp.2013.05.020

Resende, L. C. A., Shi, J. K., Denardini, C. M., Batista, I. S., Nogueira, P. A. B., Arras, C., et al. (2020). The influence of disturbance dynamo electric field in the formation of strong sporadic E-layers over Boa Vista, a low latitude station in American Sector. *Journal of Geophysical Research: Space Physics*, *108*(A5), 1176. https://doi.org/10.1029/2019JA027519

Resende, L. C. A., Shi, J. K., Denardini, C. M., Batista, I. S., Picanço, G. A., Moro, J., et al. (2021). The impact of the disturbed electric field in the sporadic E (Es) layer development over Brazilian Region. *Journal of Geophysical Research: Space Physics*, *126*(12), e2020JA028598. https://doi.org/10.1029/2020JA028598

Santos, A. M., Abdu, M. A., Souza, J. R., Sobral, J. H. A., & Batista, I. S. (2016). Disturbance zonal and vertical plasma drifts in the Peruvian sector during solar minimum phases. *Journal of Geophysical Research: Space Physics*, *121*(3), 2503–2521. https://doi.org/10.1002/2015JA022146

Shue, J. H., Song, P., Russell, C. T., Steinberg, J. T., Chao, J. K., & Zastenker, G. (1998). Magnetopause location under extremes solar wind conditions. *Journal of Geophysical Research*, *103*(17), 691–697. https://doi.org/10.1029/98JA01103

Singh, R., & Sripathi, S. (2020). A statistical study on the local time dependence of equatorial spread F (ESF) irregularities and their relation to low-latitude Es layers under geomagnetic storms. *Journal of Geophysical Research: Space Physics*, *125*(1), e2019JA027212. https://doi.org/10.1029/2019JA027212

Sobral, J. H. A., Abdu, M. A., Yamashita, C. S., Gonzalez, W. D., Gonzalez, A. C., Batista, I. S., et al. (2001). Responses of the low-latitude ionosphere to very intense geomagnetic storms. *Journal of Atmospheric and Solar-Terrestrial Physics*, *63*(9), 965–974. https://doi.org/10.1016/S1364-6826(00)00197-8

Stephan, A. W., Colerico, M., Mendillo, M., Reinisch, B., & Anderson, D. (2002). Suppression of equatorial spread-F by sporadic E. *Journal of Geophysical Research*, *107*(A2), 1021. https://doi.org/10.1029/2001JA000162

Tsurutani, B. T., Gonzalez, W. D., Gonzalez, A. L., Tang, F., Arballo, J. K., & Okada, M. (1995). Interplanetary origin of geomagnetic activity in the declining phase of the solar cycle. *Journal of Geophysical Research*, *100*(A11), 717–733. https://doi.org/10.1029/95JA01476

Whitehead, J. (1961). The formation of the sporadic-E in the temperate zones. *Journal of Atmospheric and Terrestrial Physics*, *20*(1), 1155–1167. https://doi.org/10.1016/0021-9169(61)90097-6